ACS APPLIED MATERIALS & INTERFACES

Article

Boronic Acid Moiety as Functional Defect in UiO-66 and Its Effect on Hydrogen Uptake Capacity and Selective CO2 Adsorption: A Comparative Study

Mustafa Erkartal, and Unal Sen

ACS Appl. Mater. Interfaces, **Just Accepted Manuscript** • DOI: 10.1021/acsami.7b16937 • Publication Date (Web): 19 Dec 2017

ACS Publications

ACS Applied Materials & Interfaces is published by the American Chemical Society.
1155 Sixteenth Street N.W., Washington, DC 20036

Boronic Acid Moiety as Functional Defect in UiO-66 and Its Effect on Hydrogen Uptake Capacity and Selective CO_2 Adsorption: A Comparative Study

Mustafa Erkartal[1,2,*], Unal Sen[3,§,*]

[1]Department of Materials Science and Nanotechnology Engineering, Abdullah Gül University, 38080, Kayseri, Turkey

[2]Siren Ultrasonik Research and Development, Erciyes Teknopark, 38039, Kayseri, Turkey

[3]Department of Mechanical Engineering, Abdullah Gül University, 38080, Kayseri, Turkey[§]

[§]former affiliation until August 2016

*Corresponding Author(s)

E-mail: mustafa.erkartal@agu.edu.tr

E-mail: senunal@gmail.com

Keywords: metal-organic frameworks (MOFs), UiO-66, boronic acid, hysteric adsorption, hydrogen uptake

Abstract

Herein, we use linker fragmentation approach to introduce boronic acid moieties as functional defects into Zr-based metal–organic frameworks (UiO-66). Our findings show that the amount of permanently incorporated boronic acid containing ligand is directly dependent on the synthesis method. The accessible boronic acid moieties in the pore surfaces significantly improve the hydrogen uptake values, which are 3.10 wt% and 3.44 wt% at 21 bar, 77 K for DMF/H_2O and DMF/HCl synthesis methods, respectively. Also, CO_2 selectivity of the resulting MOFs over N_2 and CH_4 significantly increases due to the quadrupolar interaction between active surfaces and CO_2 molecules. To the best of our knowledge, both hydrogen storage and selectivity of CO_2 for UiO-66 are the highest reported values in the literature to date. Furthermore, another striking result emerged from the high pressure hydrogen uptake isotherms is the direct correlation between defects and hysteric adsorption behavior, which may be resulted in shifting from rigidity to flexibility of framework due to the uncoordinated sites.

1. Introduction

Metal–organic frameworks (MOFs) are crystalline porous materials constructed from a combination of coordinatively bonded multitopic organic linkers and metal/metal cluster nodes. Unlike many other inorganic porous materials, MOFs have permanent high surface areas, tunable pore sizes, and tailorable framework architectures.[1-5] Due to such intriguing properties, MOFs have attracted tremendous attention in gas storage/separation,[6-10] catalysis,[11-12] drug delivery,[13-14] and electrochemical applications.[15-19] One of the most conspicuous features of MOFs is the modular nature - that is, their properties can be finely tuned by using a substituted organic ligand and secondary building units (SBUs).

Post-synthetic modification (PSM) has emerged as efficacious approach for fine-tuning physical and chemical properties of framework for desired applications.[20-22] Unfortunately, every so often it has been found that linker modifications bring about a significant decrease in specific surface areas and pore volumes, and generally deterioration in thermal stability of frameworks.[23-24] Alternatively, one convenient synthesis method to design MOFs with desired functional sites is mixed-ligand approach in which a parent ligand and a fragment ligand with different functional groups are employed during a synthesis. The obtained novel MOFs not only maintain the isostructure of the parent frameworks, but also they can show similar thermal and chemical stabilities comparable to parent frameworks.[25-28] Thus far, this approach has been implemented on numerous MOFs, which include MOF-5,[29] MILs,[30-31] HKUST-1,[32] ZIFs,[33] and UiO-66.[34] A few of the common outputs of all these reports can be listed as follows: (i) topology of the MOFs is maintained; (ii) depending on the functional groups of fragment ligand, frameworks gain specific properties for particular purpose, such as catalytic, sorption and electrochemical; (iii) incorporation of daughter ligands are highly affected by synthesis procedure; (iv) ratio between linkers alters the physical and chemical properties of frameworks.[25-27, 29-34]

UiO-66(Zr), consist of $Zr_6O_4(OH)_4$ clusters and terephthalic acid (BDC), has recently attracted considerable interest due to its porosity, ease of synthesis, low cost, and most importantly its high thermal, mechanical and chemical stability.[35] In spite of this

attractiveness, reported specific gas adsorption values for unfunctionalized and/or defect free UiO-66 are very modest.[36] Lillerud and co-workers have addressed this fact to its relative low surface area and lack of functional groups on BDC linkers.[37] On the other hand, Zr_6–MOFs are very tolerant of structural defects, which make them ideal candidate for synthesizing mixed-ligand MOFs.[38-39] A growing body of literature has examined the creation and controlling of missing linker/cluster defects in UiO-66 and functionalizing of UiO-66 by mixing-ligand approach. In most of these studies, defects and heterogeneities noticeably enhance the adsorption properties and catalytic activities.[37-41]

In this study we report the incorporation of active boronic acid moieties into UiO-66 by mixed-ligand approach. To this end, an inexpensive commercially available 4-carboxyphenylboronic acid (CPB) was utilized as fragment ligand to obtain the corresponding mixed-ligand MOF, UiO-66B. Since CPB is structurally very similar to BDC -rodlike ligand structure, their lengths, etc.- it can be easily incorporated into the framework without/less distortions and will provide the desired functionality to the framework owing to the uncoordinated boronic acid group on it. That is, the active boronic acid moieties in the pore surfaces may increase the hydrogen uptake capacity of the resulting MOF due to the hydrogen affinity of boron. Furthermore, the quadrupolar interaction between boronic acid groups and CO_2 molecules can enhance the CO_2 capture capabilities of the resulting MOFs.

2. Experimental Section

2.1. Materials

Zirconium (IV) chloride ($ZrCl_4$, 99.5%), terephtalic acid (BDC, 98%), 4-carboxyphenyl boronic acid (CPB, 97%) were purchased from Alfa Aesar. Hydrochloric acid (HCl, fuming 37%), dimethylformamide (DMF), ethanol, deuterium oxide (D_2O, 99.9%) were purchased from Merck. Benzoic acid (99.5%) and sodium hydroxide (98%) were purchased from Sigma Aldrich. All chemicals were used without further purification.

2.2. Synthesis of MOFs

In the literature, there are several successful synthetic methods for the synthesis of defect-free and defective UiO-66 type MOFs. Among them, two different procedures

were chosen for this study to implement mixed-ligand approach. Through synthesize of the first set, the route used is as reported by Chavan *et al* with a small modification.[34] The precursors were prepared in the beakers by successively mixing DMF, $ZrCl_4$, H_2O, and linker(s) with a molar ratio of 350:1:1.3:1, respectively. The molar ratio of ligands were altered according to BDC (4.3(1-x) mmol) and CPB (4.3x mmol, x=0, 0.13, 0.25, 0.38, 0.50), and five different samples were obtained. The precursors then transferred to 200 ml screw cap bottles and placed in an isothermal oven at 100 °C for 72 h. The obtained microcrystalline product, after cooling down room temperature, separated from the mother liquid by centrifugation and washed with fresh DMF for four times. The residual solvents were removed from pores by heating the samples at 200 °C for 24 h. All characterizations were performed on these activated materials. Second set samples have been prepared following a reported route by Katz *et al*.[42] More details for both syntheses can be found in Supporting Information. Hereafter, pure phase and mixed-ligand samples for the first set are denoted by UiO-66 and UiO-66B, and for the second set UiO-66-HCl and UiO-66B-HCl, respectively.

2.3. Instrumentation for Physicochemical Measurements

Infrared spectra of all samples were collected by using Attenuated Total Reflectance Fourier Transform Spectroscopy (ATR-FTIR) on Thermo Nicolet 6700. Spectra were obtained with 4 cm^{-1} resolution between 400–4000 cm^{-1}. Powder X-ray diffraction patterns were obtained using a Rigaku Ultima-IV powder X-ray diffractometer equipped Cu-Kα radiation. Measurements were performed over a range of $2º<2\theta<50$ in 0.02 step size with a scanning rate of 1 deg/min. Thermal analysis measurements were carried out on a Setaram Labsys TG/DT system, between 25-700 ºC with a 10 ºC/min heating rate under N_2 flow. X-ray photoelectron spectroscopy (XPS) measurements were conducted using a Thermo Scientific Kα X-ray photoelectron spectrometer system. The morphologies of the obtained samples were examined by Zeiss EVO LS 10. ^{1}H NMR spectra were recorded on a Bruker 400 spectrometer (1H, 400 MHz). For a typical measurement, 20 mg powder MOF was dissolved in 1 M 600 µL $NaOH/D_2O$ stock solution. Then, the solution was sonicated for 30 minutes and held at room temperature for 24 h. Dissolved samples were filtered using PTFE filters with a pore size of 0.45 µm,

then put into NMR tube for the measurement, and ^{1}H NMR spectra were obtained by locking the sample to D_2O.

2.4. Gas Adsorption Measurements

For all measurements, about 100-200 mg of resulting MOF was transferred into tared sample holder, and then samples were degassed at 150 ºC for 15 h by Micrometrics SmartPrep. After weighed, nitrogen adsorption/desorption isotherms and other low pressure measurements for H_2, CH_4 and CO_2 were obtained on Micromeritics Tristar II Plus surface area and porosity analyzer at desired temperatures. Each measurement was carried out at least two times for the accuracy. To obtain the desired temperatures of -196 ºC, 0 ºC, and 25 ºC the dewar was filled with liquid nitrogen, ice-distilled water mixture, and distilled water, respectively. The filler rod was also used for all measurements. The post-processing calculations and derivations on isotherms were obtained using Microactive Version 2.02 software. High-pressure adsorption measurements in the range of 0-60 bar were carried out on a Micrometrics HPVA-II High Pressure Volumetric Analyzer. Typically, 250-350 mg activated sample was transferred into tared 2-cc stainless steel sample holder, and then degassed at 150 ºC for 15 h on activation port of the instrument. Afterward, the H_2 adsorption isotherms were recorded at 77 K for each sample.

3. Results and Discussion

3.1. Synthesis and Structure

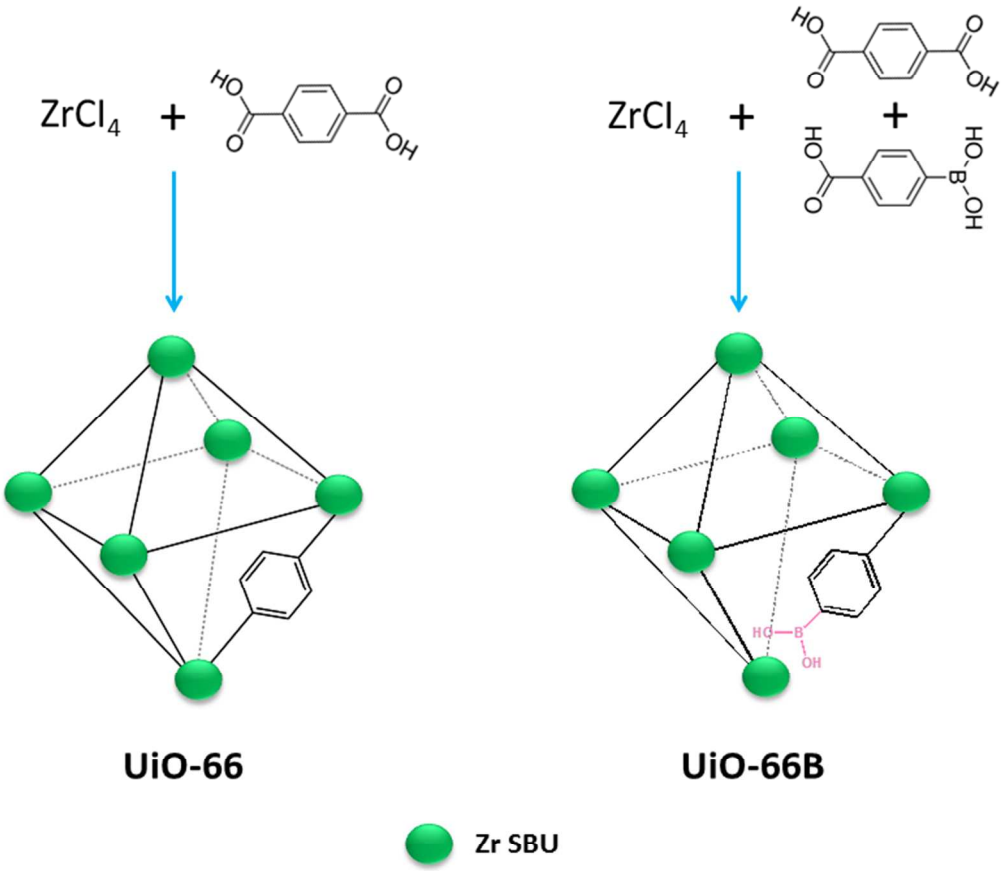

Scheme 1. Schematic presentations for synthesize procedure of pure phase UiO-66 and mixed-ligand UiO-66B

The phase pure UiO-66 and mixed-ligand UiO-66B MOFs were synthesized from $ZrCl_4$ and a mixture of BDC (parent ligand) and CPB (fragment ligand) via hydrothermal synthesis method (Scheme 1).[34] In order to seek the maximum incorporation of boronic acid into framework without changing crystal structure of UiO-66, different feed ratios of BDC to CPB were employed. Changes in crystal structure and crystallinity of the mixed ligand MOFs with BDC/CPB feed ratios from 0.87:0.13 to 0.50:0.50 were investigated by using PXRD technique. The XRD patterns of all samples are consistent with the simulated and experimental pure phase pattern of UiO-66, which means UiO-66B mixed ligand MOFs crystallized in the same structure as the pure phase UiO-66, namely the

obtained MOFs are isostructure of the parent framework (Figure 1).[31, 34] On the other hand, the diffraction peaks in the pattern are broadened and weakened as the CPB content increases. It is very likely that the crystallinity of the frameworks decreases due to the uncoordinated sites with an increasing boronic acid moiety in the framework. [31] However, in the MOFs synthesized using the HCl acid, there is no change in the XRD peaks despite the relatively higher CPB ligand (BDC/CPB, 0.25:0.75) and is compatible with the pure phase UiO-66 structure (Figure S3) The main reason for this is the introduction of much less CPB ligand, which is confirmed by ^{1}H NMR data, in the synthesis of the MOF with HCl procedure. In addition, SEM micrographs have demonstrated that there is no significant change in crystal morphologies with the incorporation of CPB into structures (Figure S4).

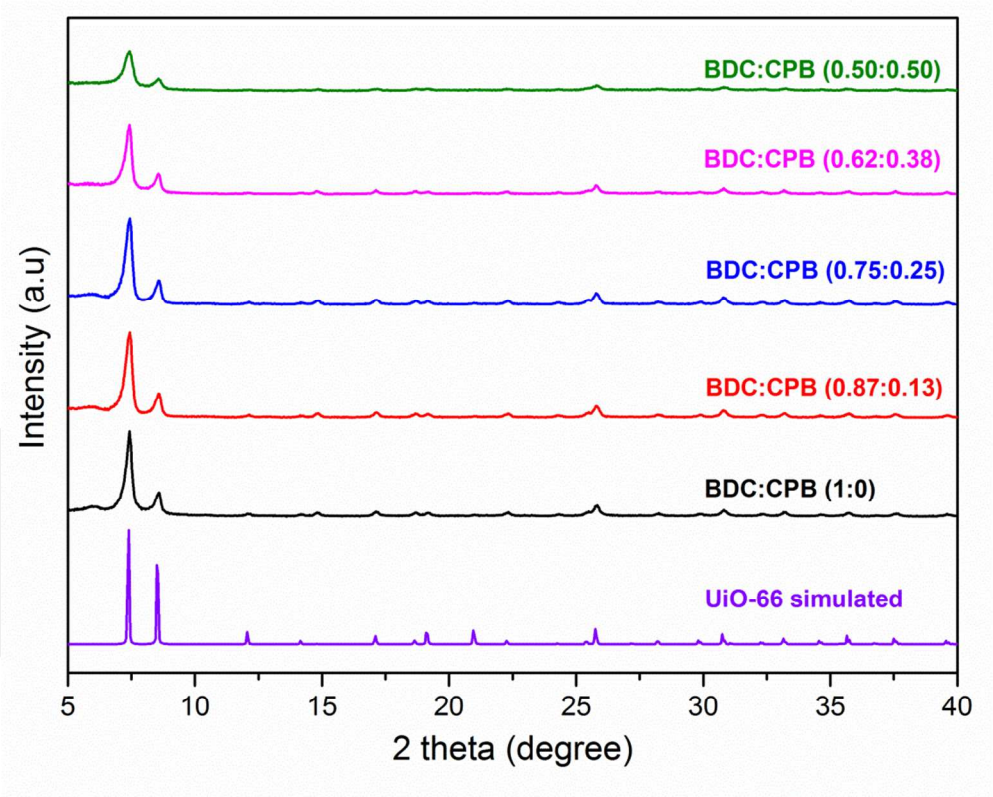

Figure 1. PXRD patterns of simulated UiO-66, pure phase UiO-66 and mixed ligand UiO-66B in different feed ratios of BDC to CPB from (0.87:0.13) to (0.50:0.50).

To qualitatively and accurately ascertain the amount of CPB in mixed ligand synthesized UiO-66, ^{1}H NMR spectra were recorded. Our steps proceed very much in the same way as described by Lillerud.[37] A certain amount of all five samples in the series and small amount of BDC and CPB ligands were digested in 1 M NaOH/D_2O. In this deuterated digestion medium, MOFs were disassembled, organic components in the frameworks (linkers, residual solvents, etc.) dissolved in the medium while metallic parts were precipitated. It is apparent from Figure 2a that BDC has a singlet at 7.69 ppm corresponding to four equivalent non-labile protons on its benzene ring. On the other hand, CPB have multiplets at around 7.58 and 7.35 ppm assigning to unsymmetrical distinct two protons (labeled H_a and H_b) for each peaks. As can be evidently seen in Figure 2b, the peaks belonging to the both ligands appear on the mixed-ligand MOFs spectra, as well the relative intensity of the peaks assigning to the CPB ligands increase with the increasing feed ratio of this ligand (Figure 2c). The molar ratios of used ligands are determined by the integrating of ^{1}H NMR spectra. For BDC/CPB feed ratios of 0.87:0.13, 0.75:0.25, 0.62:0.38, and 0.50:0.50, calculated BDC/CPB ratios through the integration of ^{1}H NMR spectra are 0.93:0.07, 0.80:0.20, 0.74:0.26, and 0.69:0.31, respectively (see Supporting Information for calculation details). It is crucial to note that the BDC/CPB ratios in MOFs do not fully match up with the ones in feed, and rather the incorporation of CPB into the frameworks is nigh on saturation at a BDC/CPB feed ratio of 0.50:0.50 (Figure 2d). Additionally, the NMR spectra of all samples include two singlets at 8.24 and 2.08 ppm which are assigning to formate and dimethylamine come from the hydrolysis of DMF.[37,43] Further investigation revealed that synthesis conditions significantly affect the incorporation of CPB into the framework. In this context, by the integration of those ^{1}H NMR spectra of UiO-66B-HCl it has been found that CPB ligands were less incorporated into the crystal structure compared with DMF/H_2O synthesis (Table S4). This would appear to indicate that the coordinated amount of CPB ligands in the frameworks are strongly depends on the synthesis conditions and that CPB was veritably incorporated into the frameworks rather than occluded in pores. Our results are in line with previous finding in the literature reported by Zhu and Lillerud.[31,34,37]

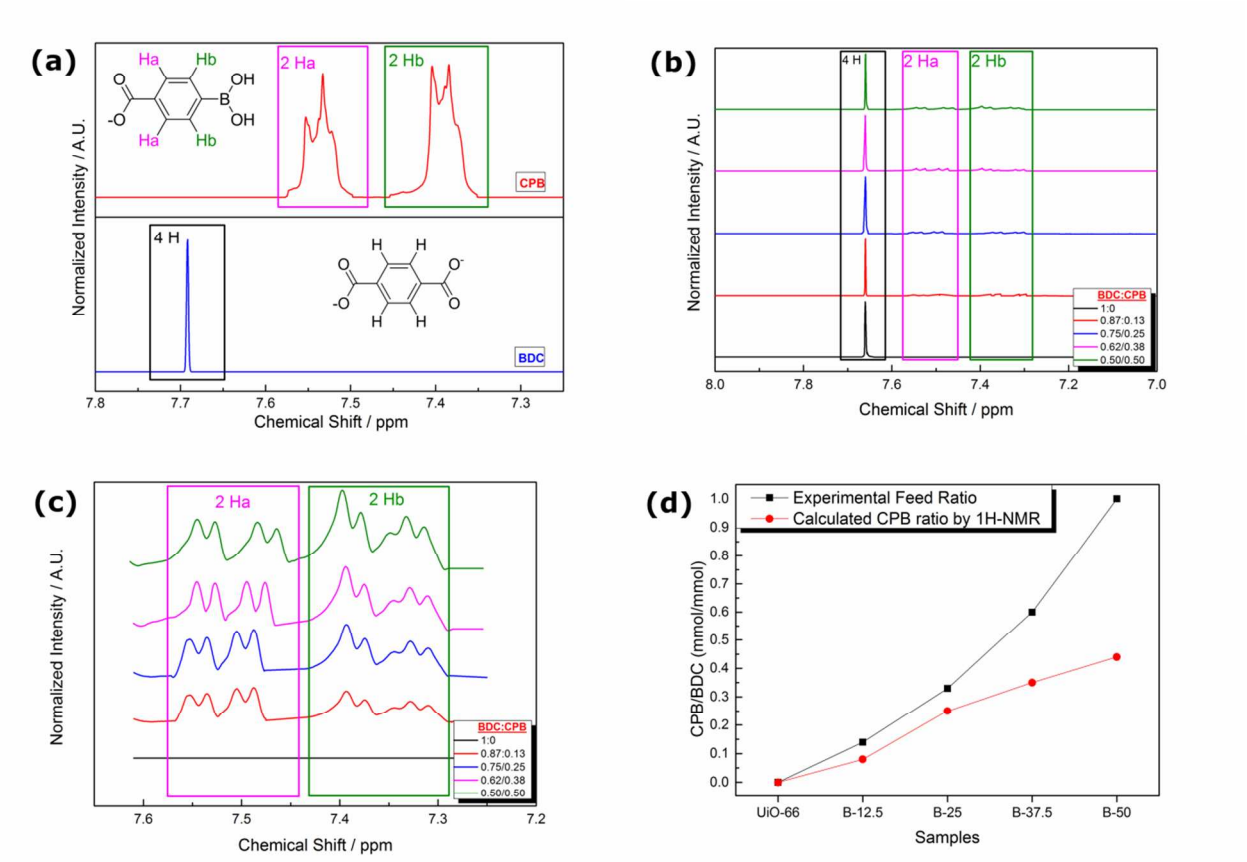

Figure 2. (**a**) Comparison of ^{1}H NMR spectra for CPB and BDC ligands. (**b-c**) ^{1}H NMR spectra obtained on the samples synthesized by DMF/H2O procedure. (**d**) Comparison of experimental feed ratio of CPB and calculated CPB ratio by ^{1}H NMR.

We also measured the XPS spectra of all synthesized MOFs for further investigation of chemical changes in their structures by incorporation of CPB. Figure 3 shows the typical wide scan XPS survey and high resolution (Zr and O) narrow scans. As shown in Figure 3a, the survey spectra revealed the existence of Zr, C, O, and N atoms in all structures.[44-46] Unfortunately, we were unable to see the presence of B atom in the surveys due to the fact that strong Zr3d (183.5/185.9 eV) loss feature strappingly overlaps the B1s (187.2 eV) region, and also B1s peak has very low sensivity.[31,47] However, according to the high resolution narrow scan spectra of Zr atom presented in Figure 3b, the binding energies of Zr3d shifts to lower values as the portion of CPB

increases in the MOFs, evincing the alterations in the chemical environments of this element. Binding energy depends on shielding effect triggered by the electron density around atoms. Therefore, the shift to lower values in the binding energy of Zr3d (from 185.91/183.57 eV to 185.33/182.99 eV) could be ascribed to the enhanced electron density around Zr atoms, which may arise out of the weaker interactions between boronic acid moieties and Zr-O clusters, and uncoordinated Zr nodes.[44-46]

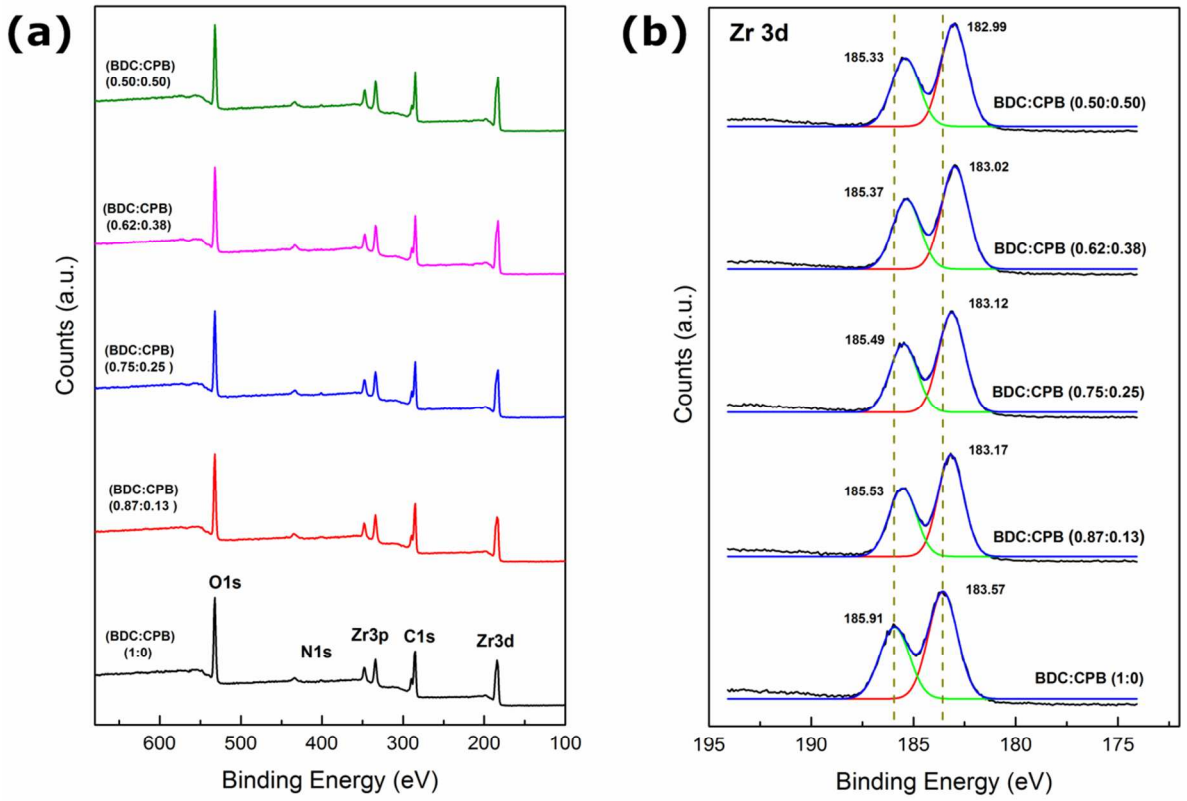

Figure 3. (**a**) XPS survey spectra of pure phase UiO-66 mixed ligand UiO-66B in different feed ratios of BDC:CPB from (0.87:0.13) to (1:1). (**b**) The enlarged Zr 3d XPS spectra of pure phase UiO-66 mixed ligand UiO-66B in different feed ratios of BDC to CPB from (0.87:0.13) to (0.50:0.50).

In order to probe the thermal stabilities of the resulting MOFs, thermogravimetric analysis was carried out for each sample. According to obtained thermograms, boronic acid containing UiO-66Bs are as stable as pure-phase UiO-66, and all of them have mainly three weigh loss step: (i) first weight loss of 5 wt% up to 100 ºC due to remaining residual solvent in the pores, (ii) second weight loss of 20 wt% up to 300 ºC is assigned to the dehydroxylation of the zirconium oxo-clusters, (iii) the last weight loss at around 500 ºC (slightly differs for each sample) is ascribed to the decomposition of frameworks (Figure S10-11).[34,37] As expected an increasing of CPB in the frameworks resulted in a decreasing in thermal stability because of the reducing of crystallinity.

Additionally, we recorded the FTIR spectra for all resulting MOFs to explore the intermolecular interaction in the frameworks. Although some characteristics absorption peaks of BDC and Zr-(μ3)O, such as at around 1390 cm^{-1} and 680 cm^{-1} respectively,[35,48] coincide with the characteristic absorption peaks of CPB, a relatively increase intensity of peaks at around 1380 cm^{-1},1000 cm^{-1} and 660 cm^{-1}, which are assigned to B-O stretching mode, B-C stretching mode and, the BO_2 out-of-plane deformation mode, respectively, were observed (Figure S6-9).[47, 49]

3.2. Gas Adsorption and Selectivity

To assess the textural parameters of prepared samples, nitrogen adsorption/desorption isotherms were collected. Figure 4a shows nitrogen sorption isotherms measured at 77 K on the samples which are synthesized by DMF/H_2O procedure. Before the adsorption/desorption experiments, all samples were activated 150 ºC for 15 h under dynamic vacuum. All samples exhibited type-I isotherm, which revealed the microporous nature of the MOFs.[35] This result has further strengthened our confidence in the following issues: (i) the introduction of CPB into UiO-66 would not abolish the structure of parent framework; (ii) CPB has been successfully incorporated into the framework instead of occluding in the pores. The calculated BET specific surface areas of prepared materials differ by different BDC/CPB feed ratios. Thus, the calculated surface area for pure-phase UiO-66 is 1361 m^2/g, whereas for BDC/CPB feed ratios of 0.87:0.13 and 0.75:0.25, the surface areas increased to 1484 and 1526 m^2/g,

respectively. This is ascribed to defect/vacant Zr nodes as a result of non-coordinated fragment ligands. However, the further increase in CPB feed ratio resulted in a dramatic decrease in BET surface areas of obtained samples. Also, the pore size distribution, obtained by NLDFT method, presents that the small pore diminished by the increasing of CPB content in the frameworks (Figure 4b.) The most likely cause of this situation can be explained as follows: Up to certain BDC/CPB ratio (here 0.75:0.25), uncoordinated sites can expand the pores by combining small pores, which lead to an increase in pore volume and BET surface area of the framework. Nevertheless, when this point is exceeded, less coordinated ligands become unable to support the whole framework, just as a small number of columns cannot support a building, some pores collapse.[34, 38] This results in a decrease of pore volume, BET surface area and crystallinity as confirmed by XRD pattern. Additionally, for BDC/CPB feed ratios of 0.75:0.25, one of the highest BET surface areas was achieved with HCl synthesis procedure in the literature: its BET surface area is 1752 m^2/g. The similar surface area trend was observed in the material obtained with HCl procedure as obtained by other method.

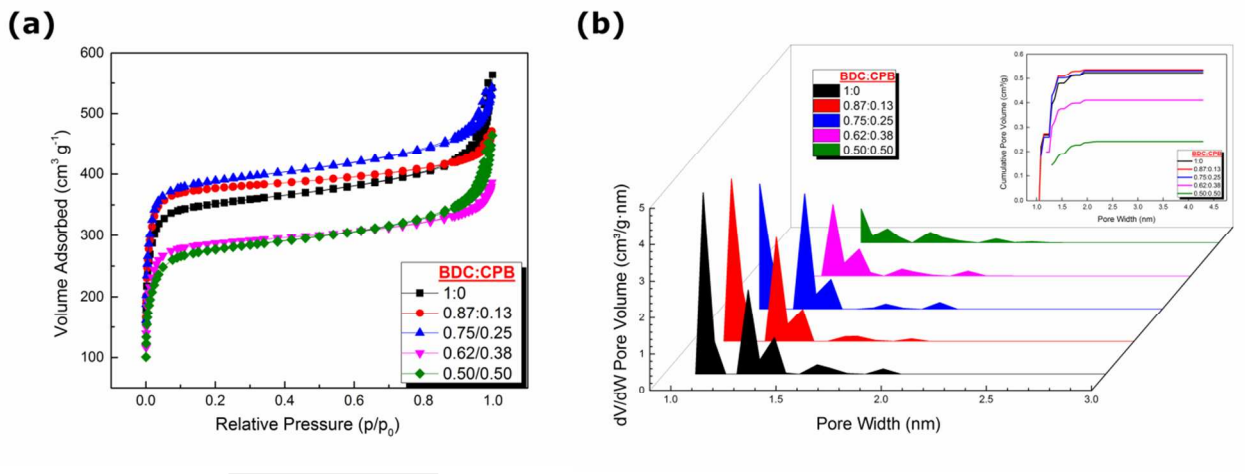

Figure 4. (**a**) N_2 adsorption isotherms of pure phase UiO-66 mixed ligand UiO-66B in different feed ratios of BDC:CPB from (0.87:0.13) to (1:1) at 77K. (**b**) NLDFT pore size distributions derived from N_2 adsorption isotherms of resulting samples.

In order to explore the hydrogen storage properties of obtained samples, low pressures and high pressures H_2 isotherms were collected at 77 K by volumetric measurement

method. Figure 5a shows the H_2 adsorption properties of the obtained samples with DMF/H_2O synthesis up to 1 bar at 77 K. According to these isotherms, while the pure phase UiO-66 reaches 1.32 wt % H_2 uptake capacity at 1 bar and 77 K, this value is 1.58 wt% for the sample with BDC/CPB feed ratios of 0.87:0.13. The high pressure H_2 uptake isotherms of these samples have almost the same adsorption trends as in low H_2 adsorption measurements (Figure 5b). In this case, pure phase UiO-66 reaches a maximum uptake of 2.38 wt% at 21 bar and 77 K and has fully reversible adsorption process. These values satisfactorily correlate with the previous finding for UiO-66 in the literature.[36] However, the sample with BDC/CPB feed ratios of 0.87:0.13 attains a maximum uptake of 3.10 wt% at 21 bar and 77 K. The most striking observation emerged from the high pressure hydrogen adsorption isotherms is hysteric adsorption behaviors of the samples with boronic acid moiety. In the literature hysteric adsorption behavior are generally attributed to flexible MOFs, this behavior is rarely reported in the adsorption of nonpolar molecules such as hydrogen and methane.[50-52] The more interesting point here is that; non-defective and pure phase UiO-66 exhibits fully reversible isotherm whereas defective samples have hysteric adsorption property.[36] This result motivated us to examine high pressure hydrogen uptakes of UiO-66 obtained with other defective synthesis method in the literature. To this end, high pressure H_2 isotherms of pure phase UiO-66 and BDC/CPB mixed ligand UiO-66 synthesized by HCl recipe and also pure phase UiO-66 obtained by benzoic acid aided method were collected. Significantly, all of the defective frameworks showed hysteric adsorption behavior. A possible explanation of this property may be that decreasing coordination between metal cluster and ligands may have altered the mechanical properties of the frameworks, so that the materials may have shifted from some rigidity to flexibility.[53] We aware that it is not possible to completely illuminate the origin of this behavior with obtained data and to better understand how missing linkers, missing clusters and heterogeneity defects affect the mechanical properties of the framework and how they change the high pressure adsorption isotherms, detailed and in-depth study is required. Additionally, although a linear relationship is usually established between the hydrogen uptake values and the surface areas of the materials, our study provides indisputable evidence for how important heterogeneity and type of it is on hydrogen uptake of the

frameworks. For instance, the BET surface area of BDC:CPB (0.75:0.25) sample synthesized with HCI procedure was the highest value among all materials, and the maximum hydrogen adsorption value for this material was 3.28 wt% at 24 bar, 77 K. Conversely, the material exhibiting the maximum hydrogen adsorption capacity is BDC: CPB feed ratios of 0.25:0.75, with a BET surface area of 1512 m^2/g and a hydrogen storage capacity of 3.44 wt%. This value is considerably higher than the defective UiO-66 containing benzoic acid which does not have functional group on it. Table 1 summarizes and compares the hydrogen adsorption and desorption values of all samples obtained in this study. An important implication of these findings is that the attractive forces between uncoordinated boronic acid moiety in the pore surfaces and H_2 molecules can increase the hydrogen uptake capacity of MOF. In addition, for all high pressure H_2 adsorption isotherms, sorption reaches a maximum and then decreases as the pressure increases. This phenomenon is a result of increasing density of hydrogen gases in the pores at elevated pressures.

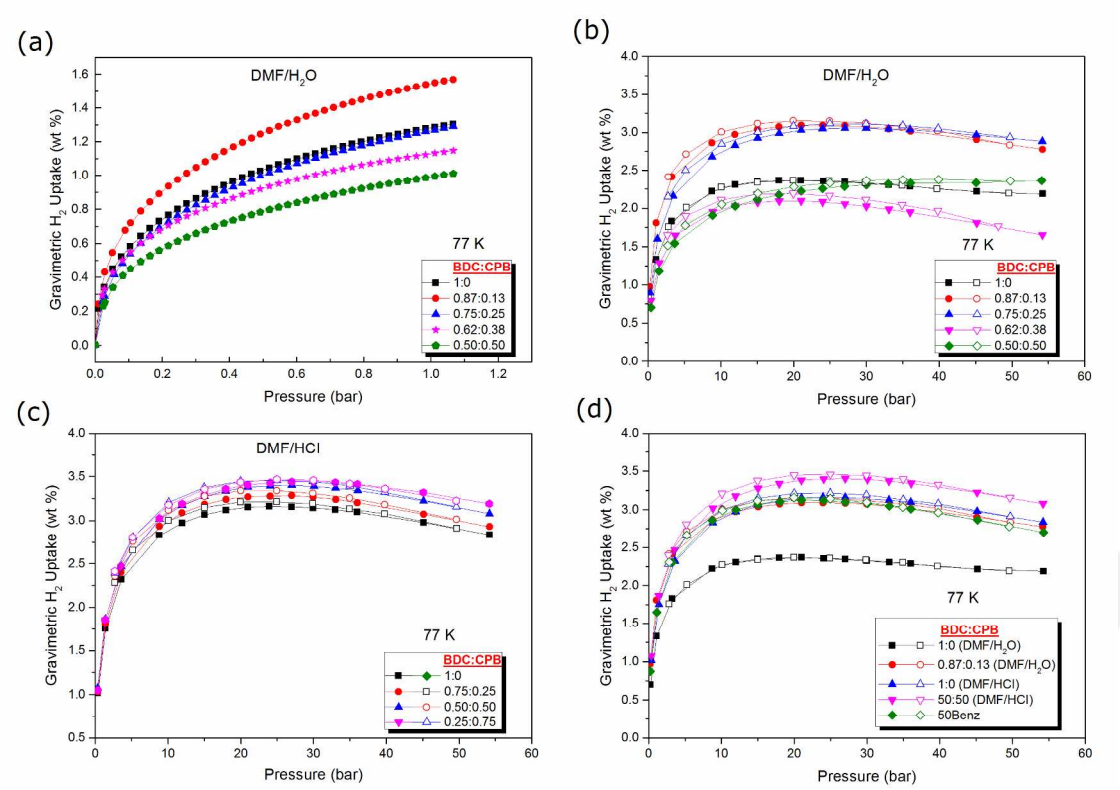

Figure 5. (**a**) The low pressure hydrogen uptake isotherms of UiO-66 and UiO-66B MOFs at 77K. (**b**)The high pressure hydrogen uptake isotherms of UiO-66 and UiO-66B at 77K (**c**) The high pressure hydrogen uptake isotherms of UiO-66-HCl and UiO-66B-HCl at 77K (**d**) A comparison for the high pressure hydrogen uptake isotherms of obtained in this study. (solid and open data represent adsorption and desorption, respectively)

Table 1. Summary of BET surface area, pore volume, max H_2 uptake capacity, IAST CO_2/N_2 and CO_2/CH_4 selectivity of all samples obtained in this study.

Solvent/ Modulator	BDC:CPB	BET SA (m^2/g)	Pore Volume (cm^3/g)	Max. H_2 adsorption value (wt %)	Max. H_2 desorption value (wt%)	CO_2/N_2 Selectivity ($S_{CO2/N2}$)	CO_2/CH_4 Selectivity ($S_{CO2/CH4}$)
DMF/Water	1:0	1361	0.49	2.38	2.38	26.6	6.5
DMF/Water	0.87:0.13	1484	0.54	3.10	3.15	27.2	6.2
DMF/Water	0.75:0.25	1526	0.53	3.06	3.11	27.4	7.2
DMF/Water	0.62:0.38	1140	0.41	2.10	2.19	34.6	9.6
DMF/Water	0.50:0.50	1061	0.24	2.32	2.32	74.9	14.1
DMF/HCl	1:0	1640	0.63	3.16	3.22	21.8	5.9
DMF/HCl	0.75:0.25	1752	0.65	3.28	3.34	21.8	6.1
DMF/HCl	0.50:0.50	1577	0.61	3.40	3.46	19.4	6.3
DMF/HCl	0.25:0.75	1512	0.59	3.44	3.47	17.8	5.5
DMF/(50)Benz	----------	1524	0.55	3.12	3.15	20.0	6.0

Figure 6 shows low pressure adsorption isotherms of pure N_2, CO_2, and CH_4 at 298 K for UiO-66B series resulting MOFs. As can be seen from these isotherms, a slight enhancement was recorded with incorporation of CPB into the framework. The sample with the feed ratio of BDC:CPB (0.87:0.13) shows the highest CO_2 and CH_4 uptake of 2.6 and 0.38 mmol/g, respectively at 298 K and 1 bar. However, even though the BET surface area of the sample with feed ratio of BDC/CPB (0.50:0.50) is much lower than the other MOFs in the same series, it still has a considerable CO_2 uptake capacity, that is 1.77 mmol/g at 298 K and 1 bar. We also calculated the selective CO_2 adsorption upon N_2 and CH_4 for all of the samples by using the ideal adsorbed solution theory (IAST) model.[54-56] Table 1 summarizes the calculated IAST selectivities for 15:85 CO_2/N_2 and 10:90 CO_2/CH_4 for all obtained materials in this study. The sample with highest CPB feed ratio (50:50) show the highest CO_2/N_2 and CO_2/CH_4 selectivity, which are three times and two times higher than CO_2/N_2 and CO_2/CH_4 selectivity of pure phase UiO-66, respectively. The higher selectivity values prompted us to calculate the isosteric heats of CO_2 adsorption of those samples. The derived Q_{st} values based on the adsorption isotherms recorded at 273, 298, and 313 K for pure phase UiO-66 and the sample with feed ratio of 50:50 are 27.5-22.6 and 25-22.3 kJ/mol, respectively. Based on the results, higher CO_2 selectivity of the sample with the highest CPB content implied the quadrupolar interaction between CO_2 and free boronic acid moiety in the pore surfaces.[55-56]

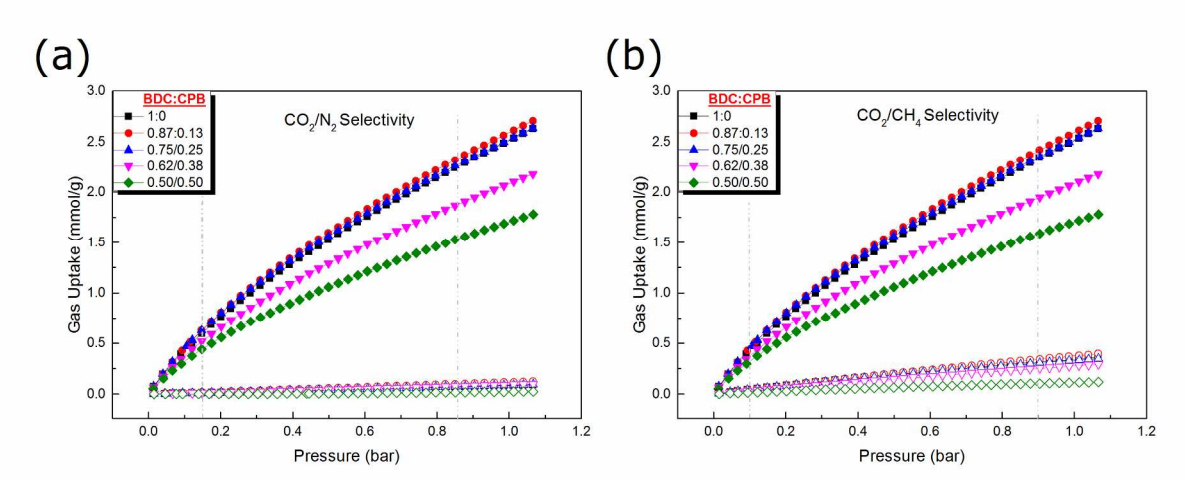

Figure 6. (**a**) The low pressure CO_2, N_2 adsorption isotherms of UiO-66 and UiO-66B MOFs at 298 K. (**b**) The low pressure CO_2, CH_4 adsorption isotherms of UiO-66 and UiO-66B MOFs at 298 K.

4. Conclusions

In summary, we investigated the incorporation of boronic acid moiety as functional defects into UiO-66 structure and its effects on gas adsorption and selectivity properties. Our findings showed that boronic acid was successfully integrated into to the frameworks, and the amount of integrated ligand is directly linked to the synthesis conditions. As hypothesized, the free boronic acid moieties in the pore surfaces considerably improve the both hydrogen uptake and CO_2 selectivity properties of the resulting MOFs. Moreover, a quite surprising observation on high pressure H_2 adsorption isotherms suggests that the increasing uncoordinated metal-ligand sites in the framework lead to hysteric H_2 adsorption due to a shift from rigidity to flexibility in the framework structure. Clearly, further research will be required to prove the correlation between the defects and hysteric guest adsorption. We think that our findings might be useful for enhancing the hydrogen adsorption properties of other Zr6 nodes containing MOFs, such as UiO-67 and NU-1000.

5. Acknowledgements

This work was supported by The Scientific and Technological Research Council of Turkey (TUBITAK) under the contract No. 114M988. M.E. acknowledges the financial support of the Techno-Initiative Capital Support Program under grant agreement no: 0257.TGSD.2015, and also thanks to Abdullah Gül University for partially fund this work.

6. Supporting Information

Supporting information includes synthetic procedures and characterizations for all samples, Figures S1-S20 and Table S1-S7.

References

(1) Eddaoudi, M.; Moler, D. B.; Li, H. L.; Chen, B. L.; Reineke, T. M.; O'Keeffe, M.; Yaghi, O. M., Modular Chemistry: Secondary Building Units as a Basis for the Design of Highly Porous and Robust Metal-Organic Carboxylate Frameworks. *Accounts Chem Res* **2001,** *34*, 319-330.
(2) Ferey, G., Hybrid Porous Solids: Past, Present, Future. *Chem Soc Rev* **2008,** *37*, 191-214.
(3) Farha, O. K.; Hupp, J. T., Rational Design, Synthesis, Purification, and Activation of Metal-Organic Framework Materials. *Accounts Chem Res* **2010,** *43*, 1166-1175.
(4) Furukawa, H.; Cordova, K. E.; O'Keeffe, M.; Yaghi, O. M., The Chemistry and Applications of Metal-Organic Frameworks. *Science* **2013,** *341*, 1230444.
(5) Bennett, T. D.; Cheetham, A. K., Amorphous Metal-Organic Frameworks. *Accounts Chem Res* **2014,** *47*, 1555-1562.
(6) Farha, O. K.; Yazaydin, A. O.; Eryazici, I.; Malliakas, C. D.; Hauser, B. G.; Kanatzidis, M. G.; Nguyen, S. T.; Snurr, R. Q.; Hupp, J. T., De Novo Synthesis of a Metal-Organic Framework Material Featuring Ultrahigh Surface Area and Gas Storage Capacities. *Nat Chem* **2010,** *2*, 944-948.
(7) Alezi, D.; Belmabkhout, Y.; Suyetin, M.; Bhatt, P. M.; Weselinski, L. J.; Solovyeva, V.; Adil, K.; Spanopoulos, I.; Trikalitis, P. N.; Emwas, A. H.; Eddaoudi, M., Mof Crystal Chemistry Paving the Way to Gas Storage Needs: Aluminum-Based Soc-Mof for Ch4, O-2, and Co2 Storage. *J Am Chem Soc* **2015,** *137*, 13308-13318.
(8) Wales, D. J.; Grand, J.; Ting, V. P.; Burke, R. D.; Edler, K. J.; Bowen, C. R.; Mintova, S.; Burrows, A. D., Gas Sensing Using Porous Materials for Automotive Applications. *Chem Soc Rev* **2015,** *44*, 4290-4321.
(9) Banerjee, R.; Phan, A.; Wang, B.; Knobler, C.; Furukawa, H.; O'Keeffe, M.; Yaghi, O. M., High-Throughput Synthesis of Zeolitic Imidazolate Frameworks and Application to Co2 Capture. *Science* **2008,** *319*, 939-943.
(10) Murray, L. J.; Dinca, M.; Long, J. R., Hydrogen Storage in Metal-Organic Frameworks. *Chem Soc Rev* **2009,** *38*, 1294-1314.
(11) Gascon, J.; Corma, A.; Kapteijn, F.; Xamena, F. X. L. I., Metal Organic Framework Catalysis: Quo Vadis? *Acs Catal* **2014,** *4*, 361-378.
(12) Farrusseng, D.; Aguado, S.; Pinel, C., Metal-Organic Frameworks: Opportunities for Catalysis. *Angew Chem Int Edit* **2009,** *48*, 7502-7513.
(13) Orellana-Tavra, C.; Marshall, R. J.; Baxter, E. F.; Lazaro, I. A.; Tao, A.; Cheetham, A. K.; Forgan, R. S.; Fairen-Jimenez, D., Drug Delivery and Controlled Release from Biocompatible Metal-Organic Frameworks Using Mechanical Amorphizationt. *J Mater Chem B* **2016,** *4*, 7697-7707.
(14) Horcajada, P.; Chalati, T.; Serre, C.; Gillet, B.; Sebrie, C.; Baati, T.; Eubank, J. F.; Heurtaux, D.; Clayette, P.; Kreuz, C.; Chang, J. S.; Hwang, Y. K.; Marsaud, V.; Bories, P. N.; Cynober, L.; Gil, S.; Ferey, G.; Couvreur, P.; Gref, R., Porous Metal-Organic-Framework Nanoscale Carriers as a Potential Platform for Drug Delivery and Imaging. *Nat Mater* **2010,** *9*, 172-178.
(15) Ramaswamy, P.; Wong, N. E.; Shimizu, G. K. H., Mofs as Proton Conductors - Challenges and Opportunities. *Chem Soc Rev* **2014,** *43*, 5913-5932.
(16) Taylor, J. M.; Dekura, S.; Ikeda, R.; Kitagawa, H., Defect Control to Enhance Proton Conductivity in a Metal-Organic Framework. *Chem Mater* **2015,** *27*, 2286-2289.
(17) Sen, U.; Erkartal, M.; Kung, C. W.; Ramani, V.; Hupp, J. T.; Farha, O. K., Proton Conducting Self-Assembled Metal-Organic Framework/Polyelectrolyte Hollow Hybrid Nanostructures. *Acs Appl Mater Inter* **2016,** *8*, 23015-23021.

(18) Erkartal, M.; Usta, H.; Citir, M.; Sen, U., Proton Conducting Poly(Vinyl Alcohol) (Pva)/Poly (2-Acrylamido-2-Methylpropane Sulfonic Acid) (Pamps)/Zeolitic Imidazolate Framework (Zif) Ternary Composite Membrane. *J Membrane Sci* **2016,** *499*, 156-163.
(19) Sheberla, D.; Bachman, J. C.; Elias, J. S.; Sun, C. J.; Shao-Horn, Y.; Dinca, M., Conductive Mof Electrodes for Stable Supercapacitors with High Areal Capacitance. *Nat Mater* **2017,** *16*, 220-224.
(20) Deria, P.; Mondloch, J. E.; Karagiaridi, O.; Bury, W.; Hupp, J. T.; Farha, O. K., Beyond Post-Synthesis Modification: Evolution of Metal-Organic Frameworks Via Building Block Replacement. *Chem Soc Rev* **2014,** *43*, 5896-5912.
(21) Burrows, A. D.; Frost, C. G.; Mahon, M. F.; Richardson, C., Post-Synthetic Modification of Tagged Metal-Organic Frameworks. *Angew Chem Int Edit* **2008,** *47*, 8482-8486.
(22) Cohen, S. M., Postsynthetic Methods for the Functionalization of Metal-Organic Frameworks. *Chem Rev* **2012,** *112*, 970-1000.
(23) Erkartal, M.; Erkilic, U.; Tam, B.; Usta, H.; Yazaydin, O.; Hupp, J. T.; Farha, O. K.; Sen, U., From 2-Methylimidazole to 1,2,3-Triazole: A Topological Transformation of Zif-8 and Zif-67 by Post-Synthetic Modification. *Chem Commun* **2017,** *53*, 2028-2031.
(24) Karagiaridi, O.; Lalonde, M. B.; Bury, W.; Sarjeant, A. A.; Farha, O. K.; Hupp, J. T., Opening Zif-8: A Catalytically Active Zeolitic Imidazolate Framework of Sodalite Topology with Unsubstituted Linkers. *J Am Chem Soc* **2012,** *134*, 18790-18796.
(25) Burrows, A. D., Mixed-Component Metal-Organic Frameworks (Mc-Mofs): Enhancing Functionality through Solid Solution Formation and Surface Modifications. *Crystengcomm* **2011,** *13*, 3623-3642.
(26) Lu, W. G.; Wei, Z. W.; Gu, Z. Y.; Liu, T. F.; Park, J.; Park, J.; Tian, J.; Zhang, M. W.; Zhang, Q.; Gentle, T.; Bosch, M.; Zhou, H. C., Tuning the Structure and Function of Metal-Organic Frameworks Via Linker Design. *Chem Soc Rev* **2014,** *43*, 5561-5593.
(27) Barin, G.; Krungleviciute, V.; Gutov, O.; Hupp, J. T.; Yildirim, T.; Farha, O. K., Defect Creation by Linker Fragmentation in Metal-Organic Frameworks and Its Effects on Gas Uptake Properties. *Inorg Chem* **2014,** *53*, 6914-6919.
(28) Ragon, F.; Campo, B.; Yang, Q.; Martineau, C.; Wiersum, A. D.; Lago, A.; Guillerm, V.; Hemsley, C.; Eubank, J. F.; Vishnuvarthan, M.; Taulelle, F.; Horcajada, P.; Vimont, A.; Llewellyn, P. L.; Daturi, M.; Devautour-Vinot, S.; Maurin, G.; Serre, C.; Devic, T.; Clet, G., Acid-Functionalized Uio-66(Zr) Mofs and Their Evolution after Intra-Framework Cross-Linking: Structural Features and Sorption Properties. *J Mater Chem A* **2015,** *3*, 3294-3309.
(29) Deng, H. X.; Doonan, C. J.; Furukawa, H.; Ferreira, R. B.; Towne, J.; Knobler, C. B.; Wang, B.; Yaghi, O. M., Multiple Functional Groups of Varying Ratios in Metal-Organic Frameworks. *Science* **2010,** *327*, 846-850.
(30) Lammert, M.; Bernt, S.; Vermoortele, F.; De Vos, D. E.; Stock, N., Single- and Mixed-Linker Cr-Mil-101 Derivatives: A High-Throughput Investigation. *Inorg Chem* **2013,** *52*, 8521-8528.
(31) Zhu, X. Y.; Gu, J. L.; Zhu, J. Y.; Li, Y. S.; Zhao, L. M.; Shi, J. L., Metal-Organic Frameworks with Boronic Acid Suspended and Their Implication for Cis-Diol Moieties Binding. *Adv Funct Mater* **2015,** *25*, 3847-3854.
(32) Liu, B. Y.; Li, Y. Y.; Oh, S. C.; Fang, Y. X.; Xi, H. X., Fabrication of a Hierarchically Structured Hkust-1 by a Mixed-Ligand Approach. *Rsc Adv* **2016,** *6*, 61006-61012.
(33) Thompson, J. A.; Blad, C. R.; Brunelli, N. A.; Lydon, M. E.; Lively, R. P.; Jones, C. W.; Nair, S., Hybrid Zeolitic Imidazolate Frameworks: Controlling Framework Porosity and Functionality by Mixed-Linker Synthesis. *Chem Mater* **2012,** *24*, 1930-1936.
(34) Chavan, S. M.; Shearer, G. C.; Svelle, S.; Olsbye, U.; Bonino, F.; Ethiraj, J.; Lillerud, K. P.; Bordiga, S., Synthesis and Characterization of Amine-Functionalized Mixed-Ligand Metal-Organic Frameworks of Uio-66 Topology. *Inorg Chem* **2014,** *53*, 9509-9515.

(35) Cavka, J. H.; Jakobsen, S.; Olsbye, U.; Guillou, N.; Lamberti, C.; Bordiga, S.; Lillerud, K. P., A New Zirconium Inorganic Building Brick Forming Metal Organic Frameworks with Exceptional Stability. *J Am Chem Soc* **2008,** *130*, 13850-13851.
(36) Chavan, S.; Vitillo, J. G.; Gianolio, D.; Zavorotynska, O.; Civalleri, B.; Jakobsen, S.; Nilsen, M. H.; Valenzano, L.; Lamberti, C.; Lillerud, K. P.; Bordiga, S., H-2 Storage in Isostructural Uio-67 and Uio-66 Mofs. *Phys Chem Chem Phys* **2012,** *14*, 1614-1626.
(37) Shearer, G. C.; Vitillo, J. G.; Bordiga, S.; Svelle, S.; Olsbye, U.; Lillerud, K. P., Functionalizing the Defects: Postsynthetic Ligand Exchange in the Metal Organic Framework Uio-66. *Chem Mater* **2016,** *28*, 7190-7193.
(38) Wu, H.; Chua, Y. S.; Krungleviciute, V.; Tyagi, M.; Chen, P.; Yildirim, T.; Zhou, W., Unusual and Highly Tunable Missing-Linker Defects in Zirconium Metal-Organic Framework Uio-66 and Their Important Effects on Gas Adsorption. *J Am Chem Soc* **2013,** *135*, 10525-10532.
(39) Yuan, S.; Qin, J. S.; Zou, L. F.; Chen, Y. P.; Wang, X.; Zhang, Q.; Zhou, H. C., Thermodynamically Guided Synthesis of Mixed-Linker Zr-Mofs with Enhanced Tunability. *J Am Chem Soc* **2016,** *138*, 6636-6642.
(40) Barkhordarian, A. A.; Kepert, C. J., Two New Porous Uio-66-Type Zirconium Frameworks; Open Aromatic N- Donor Sites and Their Post-Synthetic Methylation and Metallation. *J Mater Chem A* **2017,** *5*, 5612-5618.
(41) Lee, Y.; Kim, S.; Kang, J. K.; Cohen, S. M., Photocatalytic Co2 Reduction by a Mixed Metal (Zr/Ti), Mixed Ligand Metal-Organic Framework under Visible Light Irradiation. *Chem Commun* **2015,** *51*, 5735-5738.
(42) Katz, M. J.; Brown, Z. J.; Colon, Y. J.; Siu, P. W.; Scheidt, K. A.; Snurr, R. Q.; Hupp, J. T.; Farha, O. K., A Facile Synthesis of Uio-66, Uio-67 and Their Derivatives. *Chem Commun* **2013,** *49*, 9449-9451.
(43) Shearer, G. C.; Chavan, S.; Bordiga, S.; Svelle, S.; Olsbye, U.; Lillerud, K. P., Defect Engineering: Tuning the Porosity and Composition of the Metal-Organic Framework Uio-66 Via Modulated Synthesis. *Chem Mater* **2016,** *28*, 3749-3761.
(44) Zhu, X. Y.; Gu, J. L.; Wang, Y.; Li, B.; Li, Y. S.; Zhao, W. R.; Shi, J. L., Inherent Anchorages in Uio-66 Nanoparticles for Efficient Capture of Alendronate and Its Mediated Release. *Chem Commun* **2014,** *50*, 8779-8782.
(45) Wang, A. N.; Zhou, Y. J.; Wang, Z. L.; Chen, M.; Sun, L. Y.; Liu, X., Titanium Incorporated with Uio-66(Zr)-Type Metal-Organic Framework (Mof) for Photocatalytic Application. *Rsc Adv* **2016,** *6*, 3671-3679.
(46) Yang, J.; Dai, Y.; Zhu, X. Y.; Wang, Z.; Li, Y. S.; Zhuang, Q. X.; Shi, J. L.; Gu, J. L., Metal-Organic Frameworks with Inherent Recognition Sites for Selective Phosphate Sensing through Their Coordination-Induced Fluorescence Enhancement Effect. *J Mater Chem A* **2015,** *3*, 7445-7452.
(47) Wang, Y.; Lu, L. L.; Peng, H.; Xu, J.; Wang, F. Y.; Qi, R. J.; Xu, Z. A.; Zhang, W., Multi-Doped Carbon Dots with Ratiometric Ph Sensing Properties for Monitoring Enzyme Catalytic Reactions. *Chem Commun* **2016,** *52*, 9247-9250.
(48) Wang, C. H.; Liu, X. L.; Chen, J. P.; Li, K., Superior Removal of Arsenic from Water with Zirconium Metal-Organic Framework Uio-66. *Sci Rep* **2015,** *5*, 16613.
(49) Oh, S. W.; Weiss, J. W. E.; Kerneghan, P. A.; Korobkov, I.; Maly, K. E.; Bryce, D. L., Solid-State 11b and 13c Nmr, Ir, and X-Ray Crystallographic Characterization of Selected Arylboronic Acids and Their Catechol Cyclic Esters. *Magn Reson Chem* **2012,** *50*, 388-401.
(50) Choi, H. J.; Dinca, M.; Long, J. R., Broadly Hysteretic H-2 Adsorption in the Microporous Metal-Organic Framework Co(1,4-Benzenedipyrazolate). *J Am Chem Soc* **2008,** *130*, 7848-7850.
(51) Zhao, X. B.; Xiao, B.; Fletcher, A. J.; Thomas, K. M.; Bradshaw, D.; Rosseinsky, M. J., Hysteretic Adsorption and Desorption of Hydrogen by Nanoporous Metal-Organic Frameworks. *Science* **2004,** *306*, 1012-1015.

(52) Zhong, D. C.; Zhang, W. X.; Cao, F. L.; Jiang, L.; Lu, T. B., A Three-Dimensional Microporous Metal-Organic Framework with Large Hydrogen Sorption Hysteresis. *Chem Commun* **2011,** *47*, 1204-1206.
(53) Schneemann, A.; Bon, V.; Schwedler, I.; Senkovska, I.; Kaskel, S.; Fischer, R. A., Flexible Metal-Organic Frameworks. *Chem Soc Rev* **2014,** *43*, 6062-6096.
(54) Lee, D.; Zhang, C. Y.; Wei, C.; Ashfeld, B. L.; Gao, H. F., Hierarchically Porous Materials Via Assembly of Nitrogen-Rich Polymer Nanoparticles for Efficient and Selective Co2 Capture. *J Mater Chem A* **2013,** *1*, 14862-14867.
(55) Wang, B.; Huang, H. L.; Lv, X. L.; Xie, Y. B.; Li, M.; Li, J. R., Tuning Co2 Selective Adsorption over N-2 and Ch4 in Uio-67 Analogues through Ligand Functionalization. *Inorg Chem* **2014,** *53*, 9254-9259.
(56) He, Y. B.; Xiang, S. C.; Zhang, Z. J.; Xiong, S. S.; Wu, C. D.; Zhou, W.; Yildirim, T.; Krishna, R.; Chen, B. L., A Microporous Metal-Organic Framework Assembled from an Aromatic Tetracarboxylate for H-2 Purification. *J Mater Chem A* **2013,** *1*, 2543-2551.

TOC